


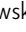
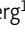
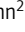
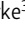



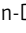
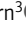





## ARTICLE

# Systematic memory B cell archiving and random display shape the human splenic marginal zone throughout life

Artur Kibler<sup>1</sup>, Bettina Budeus<sup>1</sup>, Ekaterina Homp<sup>1</sup>, Kevin Bronischewski<sup>1</sup>, Victoria Berg<sup>1</sup>, Ludger Sellmann<sup>2</sup>, Florian Murke<sup>3</sup>, Andreas Heinold<sup>3</sup>, Falko M. Heinemann<sup>3</sup>, Monika Lindemann<sup>3</sup>, Isabelle Bekeredian-Ding<sup>4</sup>, Peter A. Horn<sup>3</sup>, Carsten J. Kirschning<sup>5</sup>, Ralf Küppers<sup>1</sup>, and Marc Seifert<sup>1</sup>

**Human memory B cells (MBCs) are generated and diversified in secondary lymphoid tissues throughout the organism. A paired immunoglobulin (Ig)-gene repertoire analysis of peripheral blood (PB) and splenic MBCs from infant, adult, and elderly humans revealed that throughout life, circulating MBCs are comprehensively archived in the spleen. Archive MBC clones are systematically preserved and uncoupled from class-switching. Clonality in the spleen increases steadily, but boosts at midlife, thereby outcompeting small clones. The splenic marginal zone (sMZ) represents a primed MBC compartment, generated from a stochastic exchange within the archive memory pool. This is supported by functional assays, showing that PB and splenic CD21<sup>+</sup> MBCs acquire transient CD21<sup>high</sup> expression upon NOTCH2-stimulation. Our study provides insight that the human MBC system in PB and spleen is composed of three interwoven compartments: the dynamic relationship of circulating, archive, and its subset of primed (sMZ) memory changes with age, thereby contributing to immune aging.**

## Introduction

Memory B cells (MBCs) are generated in secondary lymphoid tissues throughout the organism, can persist for a lifetime, and have the capacity to circulate via the bloodstream (Seifert and Küppers, 2016; Weisel and Shlomchik, 2017). MBCs can further adapt in secondary immune responses (Dogan et al., 2009; McHeyzer-Williams et al., 2015; Seifert et al., 2015). The dynamics of humoral immunity and MBC generation are well understood (De Silva and Klein, 2015; Höfer et al., 2006; Mesin et al., 2016; Seifert and Küppers, 2009). However, maintenance and age-related dynamics of the human MBC pool are barely investigated.

The spleen is the largest secondary lymphoid organ and filtration system of the peripheral blood (PB; Kraal, 1992; Steiniger and Barth, 2000). It contributes to B cell maturation and maintenance, and it serves as a reservoir for human MBCs (Cerutti et al., 2013; Dunn-Walters et al., 1995; Kruetzmann et al., 2003; Mamani-Matsuda et al., 2008; Mebius and Kraal, 2005; Tangye et al., 1998). The spleen fulfills a major role in the protection from blood-borne pathogens (Kruetzmann et al., 2003; Martin et al., 2001). This protective role is fully developed at

around 2 yr of age and wanes in the elderly population. This renders both age groups, infants and elderly, susceptible to infections with polysaccharide-encapsulated bacteria, and unresponsive to many vaccination strategies (Gibson et al., 2009; Kruetzmann et al., 2003; Timens et al., 1989; Wasserstrom et al., 2008). The protective function of the spleen is essentially provided by specialized B lymphocytes, located in a histologically defined structure, the splenic marginal zone (sMZ), surrounding B cell follicles (Mebius and Kraal, 2005; Steiniger, 2015).

The human sMZ is a unique microenvironment that provides a plethora of stimuli to the residing B lymphocytes, including stromal cells providing stimulation by DLL1, B cell-activating factor (BAFF), a proliferation-inducing ligand (APRIL), and interleukins. Furthermore, B cell helper neutrophils and innate lymphoid cells contribute to the specialized microenvironment, together promoting sMZ B cell survival and proliferation, supporting plasma cell differentiation, Ig secretion, and class-switching (Magri et al., 2014; Puga et al., 2011; Sintes et al., 2017). The sMZ microenvironment imposes a priming effect onto the residing lymphocytes (Cerutti et al., 2013). Studies on

<sup>1</sup>Institute of Cell Biology (Cancer Research), University of Duisburg-Essen, Essen, Germany; <sup>2</sup>Department of Haematology, University Hospital Essen, Essen, Germany; <sup>3</sup>Institute for Transfusion Medicine, University Hospital Essen, University of Duisburg-Essen, Essen, Germany; <sup>4</sup>Division of Microbiology, Paul-Ehrlich-Institut, Langen, Germany; <sup>5</sup>Institute of Medical Microbiology, University of Duisburg-Essen, Essen, Germany.

Correspondence to Marc Seifert: [marc.seifert@uni-due.de](mailto:marc.seifert@uni-due.de).

© 2021 Kibler et al. This article is distributed under the terms of an Attribution-Noncommercial-Share Alike-No Mirror Sites license for the first six months after the publication date (see <http://www.rupress.org/terms/>). After six months it is available under a Creative Commons License (Attribution-Noncommercial-Share Alike 4.0 International license, as described at <https://creativecommons.org/licenses/by-nc-sa/4.0/>).

murine or human sMZ B cells showed their high motility within the splenic microenvironment (Arnon et al., 2013; Cinamon et al., 2008), but also recirculation to the periphery (Weller et al., 2004). In mice, sMZ B cells are considered to represent a separate lineage with biased Ig heavy chain variable (IGHV) gene repertoire and distinct, Notch2-dependent generation (Cariappa et al., 2001; Hampel et al., 2011; Martin and Kearney, 2000; Tanigaki et al., 2002; Wen et al., 2005). Murine sMZ B cells are mostly Ig-unmutated and participate in the immune surveillance of the PB, and their precursors are selected according to their B cell receptor (BCR)-signaling strength into the sMZ niche (Cerutti et al., 2013; Martin and Kearney, 2002). Murine sMZ B cells develop from transitional B cell precursors, and show integrin-mediated sMZ homing and retention, follicular shuttling, and T cell-dependent (TD) and -independent (TI) responsiveness (Cerutti et al., 2013; Martin and Kearney, 2000; Pillai and Cariappa, 2009). Human sMZ B cells share several of the murine sMZ B cell characteristics, e.g., their NOTCH2-dependent generation and enhanced responsiveness (Cerutti et al., 2013; Descatoire et al., 2014; Krutzmann et al., 2003; Magri et al., 2014; Puga et al., 2011; Scheeren et al., 2008; Song and Cerny, 2003; Wasserstrom et al., 2008).

Human sMZ B cells show a MBC phenotype, according to CD27 expression and IGHV-mutation status (Dono et al., 2000; Dunn-Walters et al., 1995; Steiniger et al., 2005; Steiniger et al., 2014; Tangye et al., 1998; Tierens et al., 1999). Moreover, human sMZ B cells show low CD23 but high CD21, CD35, and CD1c expression levels (Cerutti et al., 2013; Tangye et al., 1998; Weller et al., 2004). The human sMZ harbors two functionally distinct populations of CD27<sup>+</sup>CD21<sup>high</sup> B cells, one IgM-expressing (IgM<sup>high</sup>IgD<sup>+</sup>) and one class-switched (IgG<sup>+</sup> or IgA<sup>+</sup>) population (Colombo et al., 2013; Ettinger et al., 2007; Lettau et al., 2020; Steiniger, 2015; Tangye et al., 1998; Zhao et al., 2018). Besides the sMZ B cell subset, a substantial fraction of non-sMZ MBCs is detectable in the human spleen (Ettinger et al., 2007; Lettau et al., 2020; Tangye et al., 1998; Zhao et al., 2018). These non-sMZ MBCs consist of IgM-expressing but also class-switched MBCs in histologically defined niches (Lettau et al., 2020; Zhao et al., 2018), but likely also include MBCs circulating with the bloodstream and temporarily passing the spleen.

In humans, sMZ B cells can circulate (Bagnara et al., 2015; Weller et al., 2004), contributing to a B cell clone network spanning the whole organism, and showing clonal relation between PB, gut, bone marrow, lung, and spleen (Mandric et al., 2020; Meng et al., 2017). Analysis of human antigen-specific MBCs derived from PB and spleen from the same donor revealed uneven distribution of clonally related sequences with preferential localization in the spleen (Giesecke et al., 2014; Mamani-Matsuda et al., 2008; Meng et al., 2017). T cell- and antigen-independent diversification of the sMZ B cell repertoire occurs in infants (Weller et al., 2004; Weller et al., 2001; Weller et al., 2008; Willenbrock et al., 2005), whereas PB memory diversification occurs germinal center (GC)-dependent in adults (Budeus et al., 2015; Seifert and Küppers, 2009; Seifert et al., 2015).

A comprehensive understanding of the human splenic and particularly the sMZ B cell repertoire is limited. Our knowledge

on the age-dependent dynamics of the human splenic B cell composition and homeostasis is similarly limited. Here, we present a phenotypical, molecular, and functional characterization of paired PB- and spleen-derived MBCs from healthy human subjects, covering eight decades of life. Our data suggest that throughout life, human MBCs segregate into three distinct compartments, which differ in tissue localization, diversity, and function. The PB MBC compartment (circulating memory) is generated in secondary lymphoid tissues (including the spleen) and shaped by immune responses throughout the organism. Virtually all circulating MBC clones are archived and expanded in the spleen (archive memory). From this archive compartment, MBCs are stochastically displayed and primed in the sMZ microenvironment (primed memory), which represents a functionally distinct subset of the splenic memory archive. The three MBC compartments are interwoven by selection, retention, and recirculation dynamics that change with age, thereby shaping human B cell immunity throughout life.

## Results

### Circulating MBC, splenic non-marginal zone MBC, and sMZ B cell subsets differ in phenotype and responsiveness, and their relative abundance changes with age

The human MBC system is composed of distinct subsets and distributed throughout the organism. In this study, mature B cell subsets from PB and spleen were analyzed. Splenic B cells (prefix “s”) were distinguished into sMZ and non-sMZ B cell subsets, the latter from here on referred to as splenic IgM memory B cells (sMD27) and splenic class-switched B cells (sCSW). In detail, we distinguished naive B cells (sNaive and PB-Naive, CD23<sup>+</sup>IgD<sup>high</sup>IgM<sup>low</sup>CD27<sup>+</sup>CD21<sup>+</sup>), IgM MBCs (sMD27 and PB-MD27, IgM<sup>+</sup>IgD<sup>+</sup>CD27<sup>+</sup>CD23<sup>+</sup>CD21<sup>+</sup>), class-switched MBCs (sCSW and PB-CSW, IgG/IgA<sup>+</sup>IgM<sup>+</sup>IgD<sup>+</sup>CD27<sup>+</sup>CD23<sup>+</sup>CD21<sup>+</sup>), sMZ B cells (sMZ, IgM<sup>high</sup>IgD<sup>+</sup>CD21<sup>high</sup>CD27<sup>+</sup>CD23<sup>+</sup>), and class-switched sMZ B cells (sMZ-CSW, IgG/IgA<sup>+</sup>IgM<sup>+</sup>IgD<sup>+</sup>CD21<sup>high</sup>CD27<sup>+</sup>CD23<sup>+</sup>; Fig. 1 A and Fig. S1, A and B). B cells with CD21<sup>high</sup> phenotype did not appear as a distinct population in PB (Fig. 1 A and Fig. S1, B and E).

The validity of our gating strategy was confirmed by phenotypical differences between the individual subsets, particularly in the surface expression of CD35, CD300a, and CD1c in addition to CD21 (Fig. 1 B), showing highest expression among sMZ and sMZ-CSW B cells. Circulating and splenic non-sMZ MBCs also showed significantly different expression of further surface molecules, including CD27, CD79b, CD148, and CD35 (Fig. 1 B and Fig. S2 A). We assessed the responsiveness and proliferation capacity of sMZ and non-sMZ B cell subsets upon TD and TI type I (TI-I) stimulation (Fig. 1 D). In line with previous studies (Ettinger et al., 2007; Magri et al., 2014; Puga et al., 2011; Sintès et al., 2017), sMZ B cells responded faster and more intensely than non-sMZ MBCs, with the majority of sMZ B cell subsets showing induction of CD25 and CD80 expression after 24 h, and having undergone cell division already on day 3 (Fig. 1, C and D). In contrast, PB-derived and splenic non-sMZ B cell subsets showed reduced expression of activation markers, the former responding with significantly reduced intensity

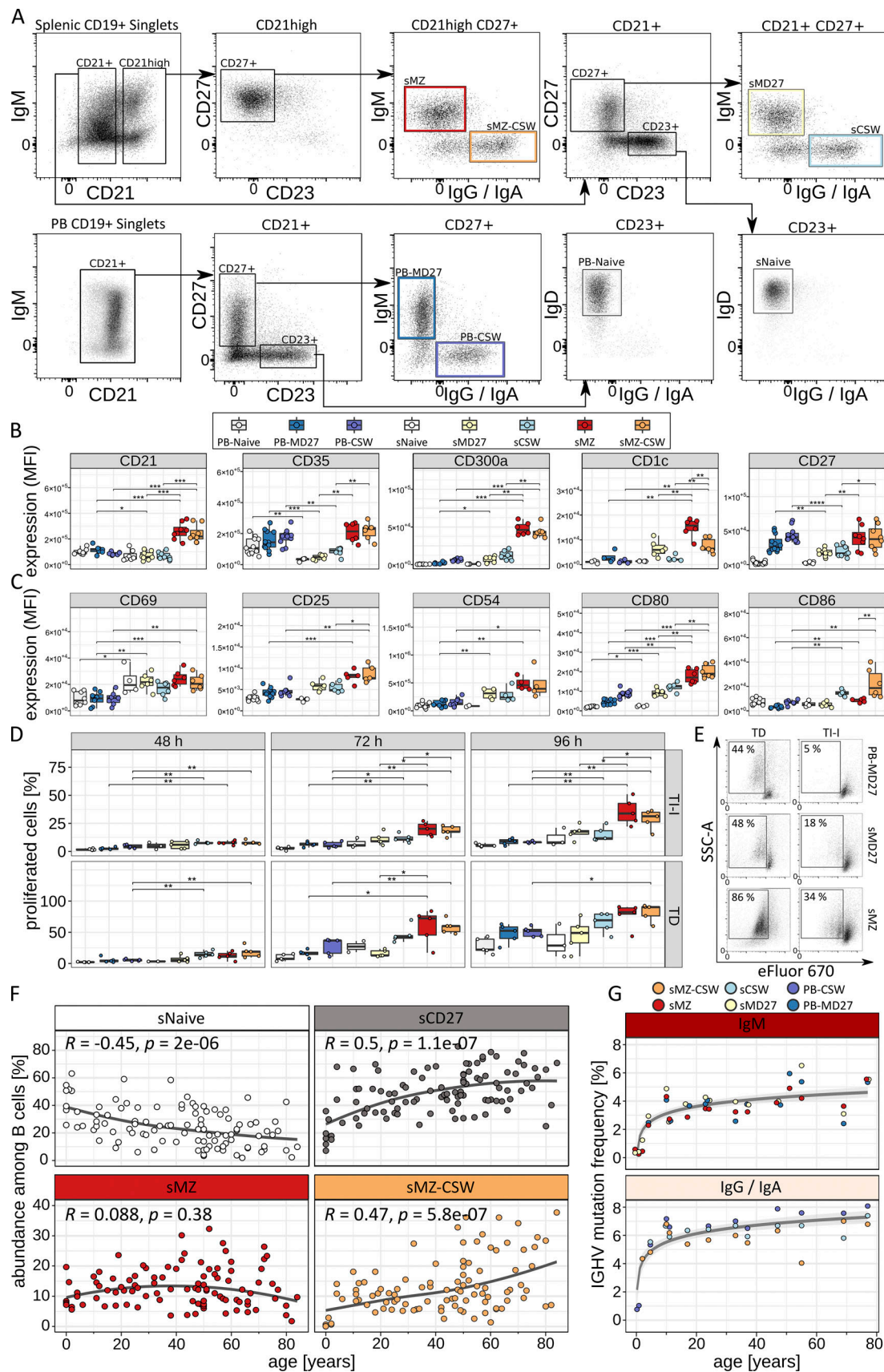


Figure 1. **Age-related changes in the human splenic B cell compartment.** (A) Gating strategy for the isolation of splenic and PB B cell subsets (for details, see Fig. S1, A and B). (B) Surface expression (median fluorescence intensity [MFI]) of selected molecules upon cell isolation without stimulation (spleen,  $n =$



4–7; PB,  $n = 7–11$ ). **(C)** Cell surface expression (MFI) of activation markers after 24 h of TD in vitro stimulation (spleen,  $n = 2–6$ ; PB,  $n = 8–11$ ). **(D)** Fraction of proliferated cells (eFluor670<sup>low</sup>) among sort-purified splenic and PB B cell subsets after 48, 72, and 96 h of TD or TI-I in vitro stimulation (spleen,  $n = 2–5$ ; PB,  $n = 4$  or 5). **(E)** Gating strategy for proliferated cells upon TD stimulation (data shown in D). **(F)** Frequency of splenic B cell subsets throughout age ( $n = 104$ ). Curves represent the smoothed conditional means, with loess fitting. Statistics denote Pearson's correlation coefficient. **(G)** IGHV-mutation frequency (median) of individual B cell subsets isolated from 17 donors. Curves in F and G represent the smoothed conditional means, with loess fitting (gray area represents CI 95%). Significance in B–D was calculated with the Wilcoxon rank-sum test (\*,  $P \leq 0.05$ ; \*\*,  $P \leq 0.005$ ; \*\*\*,  $P \leq 0.001$ ; \*\*\*\*,  $P \leq 0.0001$ ). SSC-A, side scatter area.

compared with the latter (Fig. 1 C and Fig. S2 B). This tendency was also observed in their respective proliferation capacities, particularly between class-switched B cell subsets (Fig. 1, D and E). TI-I stimulation was highly efficient among splenic B cells, but PB B cells barely responded during 96 h of TI-I stimulation. We conclude that circulating splenic MBCs and sMZ B cells differ in phenotype and response intensity (speed and type of stimulus).

Next, we determined the composition of the splenic and PB B cell compartments from 141 individuals from 0 to 89 yr of age concerning subset quantity and diversity (Table S1). Similar to PB-Naive (Fig. S1, E and F), sNaive B cells are most frequent in infants (0–1 yr of age, up to 60% of total splenic B cells), but then steadily decrease to 15% in the elderly as compared with 40% PB-Naive B cells (Fig. 1 F). Conversely, MBCs in PB and spleen are barely detectable in neonates and infants, increase during childhood, and steadily accumulate with age. MBCs account for up to 60% in the spleen and 30% in the PB of the elderly (Fig. 1 F and Fig. S1, E and F). PB-CSW, sCSW, and sMZ-CSW B cells are nearly absent from infants and children <2 yr of age but increase to adult-like levels around 2–4 yr of age and show high frequency variability in the elderly (Fig. 1 F and Fig. S1, D and G). A distinct population of sMZ B cells was already detectable in infants and young children ( $n = 8$ ; 2–24 mo; Fig. 1 F and Fig. S1 C). The average sMZ B cell frequency does not change with age, but the fraction of sMZ-CSW B cells increases from 10% in adults to an average of 20% in the elderly (Fig. 1 F and Fig. S1 C). Around 60 yr of age, the splenic B cell pool is dominated by class-switched MBC subsets (sMZ-CSW and sCSW; Fig. 1 F and Fig. S1, C–G).

We selected 17 donors, covering the age span from 0 to 77 yr, and performed deep-sequencing of IGHV gene rearrangements of sort-purified B cell subsets from spleen (sMZ, sMZ-CSW, sMD27, and sCSW) and paired PB samples (PB-MD27 and PB-CSW). We analyzed an average number of 485,000 splenic and 30,000 PB-derived B cells from each donor per subset and retrieved a total of 3,660,797 unique sequences (after quality control and collapsing identical sequences; Table S2). The average IGHV mutation frequency increases abruptly in the first years of life, and afterwards only moderately (Fig. 1 G). sMZ-CSW B cells consistently showed a slightly lower average IGHV mutation frequency compared with sCSW or PB-CSW B cells (Fig. 1 G).

Taken together, the age-related changes in the composition of the human splenic B cell compartment show the same tendencies as observed in the circulating compartment. However, in the spleen, these changes are more intense, leading to a dominance of MBCs, particularly class-switched MBCs, in the elderly.

### Throughout life, circulating B cell memory is archived in the spleen

Clonal expansions and phylogenetic analysis of IGHV gene mutation patterns can be used to reconstruct MBC dynamics (Budeus et al., 2015; Seifert and Küppers, 2009; Wu et al., 2010). We investigated the clonal relation of PB and splenic B cells (sMZ and non-sMZ) to track their diversification and distribution in our IGHV gene deep-sequencing cohort (Fig. 1 G).

The clonal abundance (fraction of sequences in clones) increases strongly in the PB during early childhood but gradually extends to the spleen until similar levels are reached at around 40 yr of age (Fig. 2 A). In all individuals, the vast majority (75–99%) of the PB MBCs have clone members in the spleen (Fig. 2 B), indicating an extensive clonal overlap between PB and splenic MBCs throughout life. Conversely, the fraction of IGHV rearrangements that cannot be assigned to clones decreases with age. This results in an overall reduced MBC repertoire diversity, which is delayed in the spleen until midlife (Fig. 2 C). Likewise, the average clone size (counting collapsed sequences deviating by at least one mutation) in the spleen shows a mild but steady increase with age (Fig. 2 D).

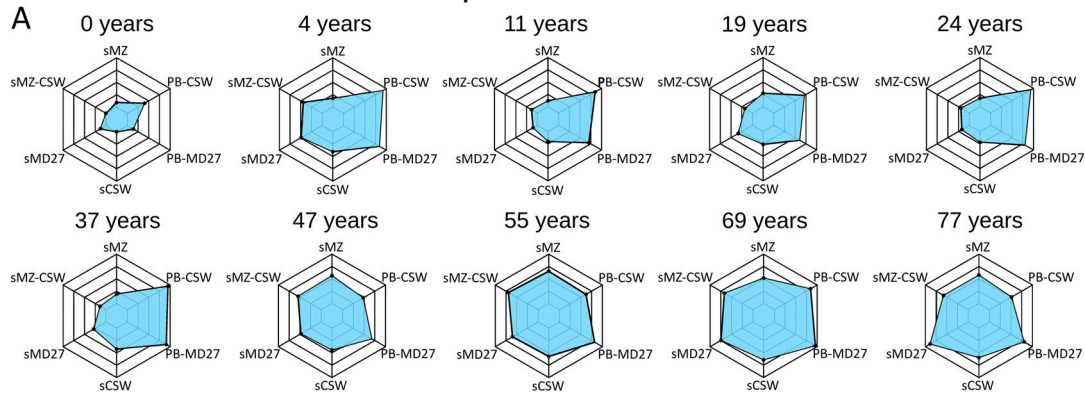
The clonal abundance and diversity of PB and splenic MBCs shift at different rates with age, and changes occur earlier in PB. Of note, the number of clones shared between tissues does not change (Fig. 2 E), but the fraction of splenic sequences in clones increases with age, mostly independent of PB (Fig. 2 F). Finally, the number of splenic clone members increases evenly, but a shift is observed around midlife (Fig. 2 G), causing a marked loss of smaller clones and diversity in the spleen (Fig. 2 C). This shift is more intense for splenic clones for which no PB sequence was detected (Fig. 2, F and G).

Taken together, our data suggest that the human spleen (including sMZ and non-sMZ B cells) not only is a reservoir for MBCs but also serves as a comprehensive archive of circulating MBC clones. Moreover, splenic MBC clone sizes appear to increase independent of the periphery.

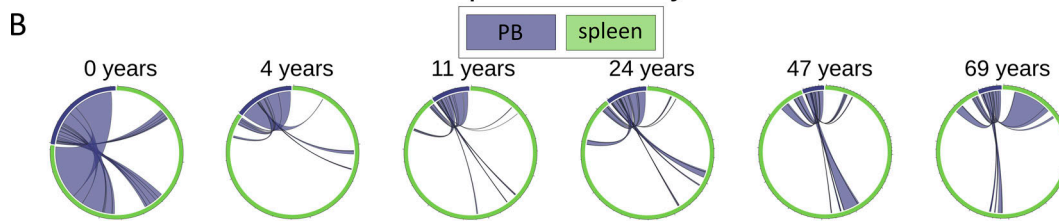
### PB and splenic clone members segregate into distinct branches

The observation that virtually all MBCs from PB have clone members in the spleen indicates that from every MBC clone egressing from secondary lymphoid tissue into the PB, eventually at least a few clone members home to the spleen. Phylogenetic analysis of clone dendrograms allows tracking of the hierarchy and dynamic generation of clone members (Meng et al., 2017; Seifert and Küppers, 2009). Hence, we performed this type of analysis on clone dendrograms consisting of PB and spleen members (shared clones). The segregation of PB- and spleen-derived clone members in dendrograms is not random,

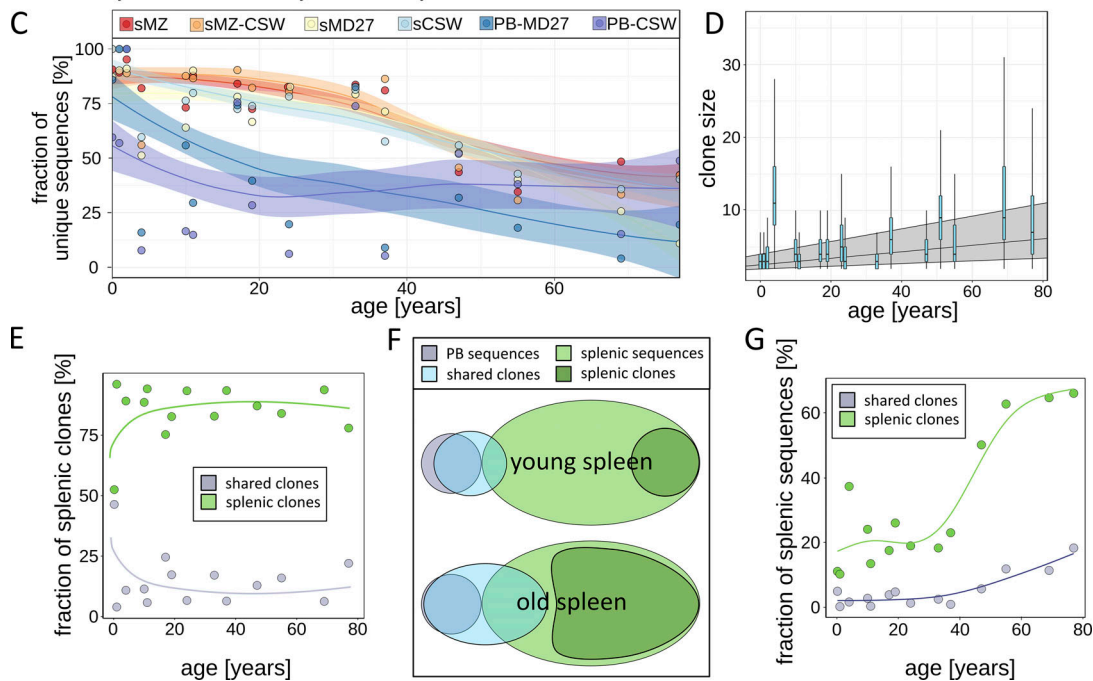
## Clonal abundance in PB and spleen



## The clonal relation of PB and splenic memory B cells

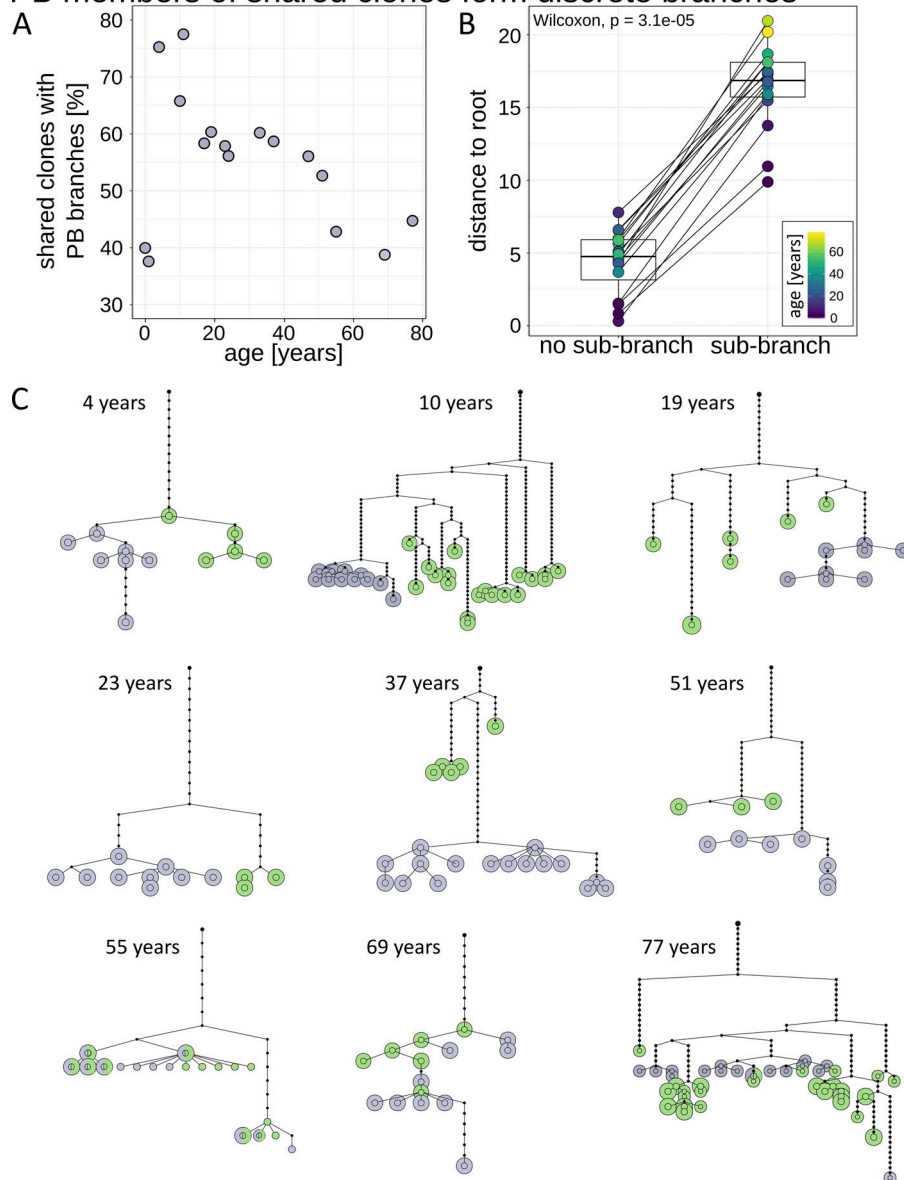


## Clonality and diversity in the spleen



**Figure 2. Clonal relation, abundance, and diversity of PB and splenic MBC subsets.** (A) Radar plot (axis range: 0% innermost tick, 100% outermost tick) depiction of the abundance of sequences assigned to clones within each subset, distributed in spleen and PB. Ten representative donors are shown ( $n = 17$ ). (B) Circos plotting of sequences shared between PB and spleen among all sequences. A selection of six representative donors is shown ( $n = 16$ ). For a display of clonal relations between PB and spleen among all sequences, see Fig. S3 A. (C) The fraction of unique sequences among PB and splenic B cell subsets from 15 donors with at least four B cell subsets available for analysis. Curves represent the smoothed conditional means, with loess fitting (gray area represents CI 95%). (D) The average clone size of all clones from each donor ( $n = 17$ ). The gray area was calculated using the quantile regression. (E) The fraction of clones locating to the spleen alone or shared with PB with age among donors with at least four B cell subsets and paired PB available for analysis ( $n = 14$ ). Curves represent the smoothed conditional means, with loess fitting. (F) Illustration of the age-related changes of clonally related sequences in spleen and PB. (G) Fraction of spleen-only or shared clones among splenic sequences from 14 donors with at least four B cell subsets and paired PB available for analysis. Curves in C, E, and G represent the smoothed conditional means, with loess fitting.

## PB members of shared clones form discrete branches



**Figure 3. Phylogenetical analysis of shared clones from PB and spleen.** (A) Fraction of shared clones with PB-derived sequences clustering in a single, discrete branch among 16 donors with paired PB and spleen cells available. (B) Displayed is the distance in terms of additional mutations to the root of the head node encompassing all nodes with PB-derived sequences represented as a boxplot ( $n = 14$ ). A sub-branch is defined as a branch consisting of PB-derived sequences exclusively. Significance was calculated using the paired samples Wilcoxon test. (C) Representative examples of genealogical trees with PB-derived sequences clustering in discrete branches (4-, 10-, 19-, 23-, 37-, and 51-yr-old donors) or intermingling of PB- (gray circles) and spleen-derived (green circles) sequences (55-, 69-, and 77-yr-old donors). Parent nodes of discrete PB branches were identified among spleen-derived sequences (4- and 69-yr-old donors) or remained elusive (10-, 19-, and 23-yr-old donors). Green circles represent spleen-derived sequences, and gray those obtained from PB. Small black dots denote postulated intermediate steps. The large black dots represent the germline sequences of the clone. Each line indicates one additional point mutation in the IGHV gene. Note that sequencing artifacts may contribute to the high intraclonal diversity observed at local nodes.

but follows a specific pattern: in early childhood, the vast majority (up to 75%) of shared clones showed a consistent separation of PB clone members in one discrete branch (Fig. 3, A and C: 4, 10, 19, and 23 yr). The frequency of clones with discrete PB branches steadily decreases with age, but still accounts for 40% of shared clones in the elderly. This separation of PB clone members within distinct branches is in 98% of the cases not preceded by a common ancestor at the branching point, hampering the identification of subset hierarchies. However, the PB sequence clusters were located significantly further downstream in the dendrograms (Fig. 3 B), indicating that on average, PB and spleen clones frequently share the early steps in Ig diversification. Thus, the spleen-resident fraction of MBCs is phylogenetically overarching the PB fraction. This is not detectable in infants but increased in children and young adults (Fig. 3, A and C). Vice versa, shared clone dendrograms that are hierarchically dominated by PB-derived sequences are

rare throughout life (<5% total), albeit most frequent among infant donors.

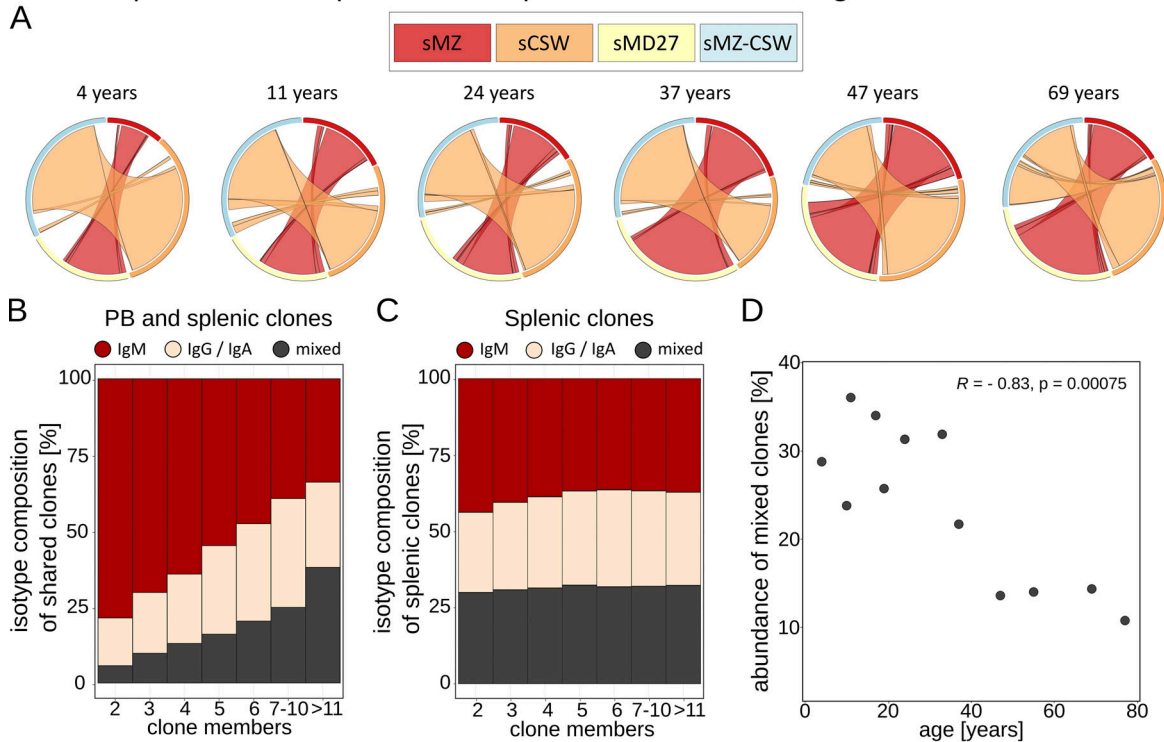
Finally, intermingling of PB and splenic clone members within a dendrogram increases with age (Fig. 3, A and C: 69 and 77 yr), supporting the idea of increased recirculation, i.e., iterative cycles of spleen egress and reentry during aging.

Taken together, the phylogenetic analysis of shared clones points to a nonrandom distribution of MBCs between PB and spleen throughout life, and PB subbranches are located significantly more downstream in dendrogram hierarchies.

#### Clonal expansion in the spleen is uncoupled from class-switching

To determine putatively distinct mechanisms of selection or diversification in the periphery and spleen, we quantified clonal expansion and relation between B cell subsets, and compared the frequency of class-switching and conserved mutations. In infants,

## Clonal expansion in the spleen is uncoupled from class-switching



**Figure 4. The different selection of circulating and archive memory.** (A) Circos plotting of clonally related sequences between sMZ and sMD27, or sMZ-CSW and sCSW subsets, respectively, is shown as ribbons, among all clonally related sequences from these four subsets. A selection of six representative donors is shown ( $n = 16$ ). For the full picture of clonal relation, see Fig. S3. (B) Clone size-dependent isotype composition among shared PB and splenic MBC clones. (C) Clone size-dependent isotype composition among splenic MBC clones, including sMZ and non-sMZ subsets. (D) Frequency of clones with mixed isotype (IgM and class-switched) among all clones, mapped according to age among 12 donors from whom IgM and class-switched B cell subsets were obtained. Pearson's correlation coefficient and statistical significance are given for a linear regression model.

expanded clones are scarce (Fig. 2), barely show Ig-mutations, and lack class-switched B cells (sMZ-CSW and sCSW; Fig. 1). Therefore, we focused on individuals >4 yr of age.

Throughout life, clonal relations within the spleen are predominantly detected between either IgM-expressing (sMZ and sMD27) or class-switched (sMZ-CSW and sCSW) B cell subsets, respectively (Fig. 4 A). About 35% of the clones in young individuals included both IgM and class-switched B cell subsets, and this fraction decreases substantially with age (Fig. 4 D). Among the shared clones between PB and spleen, the fraction of clones with IgM and class-switched members increases significantly with clone size (Fig. 4 B), as previously observed (Budeus et al., 2015). In contrast, the BCR isotype composition of the splenic MBC compartment is independent of clone size (Fig. 4 C).

Taken together, the isotype composition of clones in the circulating memory compartment is highly diverse, whereas the splenic memory compartment seems to be conserved.

#### The sMZ B cell repertoire is a stochastic selection of the total MBC compartment

We aimed at determining the distinctness of the human sMZ B cell repertoire. Our data show that sMZ B cells (CD21<sup>high</sup>) rarely belong to independent clones. In contrast, we observed a major clonal overlap of sMZ B cells and PB or splenic MBCs

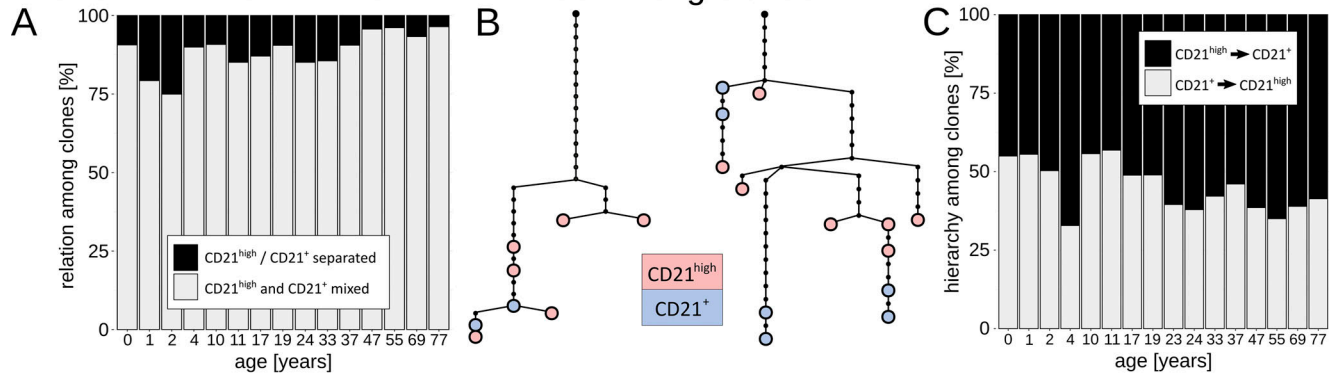
(CD21<sup>+</sup>) in all donors throughout age (Fig. 5 A). Moreover, the phylogenetic analysis did not reveal consistent hierarchical patterns, and larger clones frequently showed alternating CD21<sup>high</sup> and CD21<sup>+</sup> members in consecutive positions (Fig. 5, B and C). Among unique MBC sequences (and also when all sequences were regarded, including clonally related sequences), the average IGHV gene usage (Fig. 5 D) and distribution of complementarity-determining region III (CDRIII) length (Fig. 5 E) were nearly identical between CD21<sup>high</sup> and CD21<sup>+</sup> subsets.

Although our data lacked evidence for a specific selection or molecular distinctness of the human sMZ B cell subset, we calculated the enrichment of shared clonotypes (identical IGHV gene and at least 90% CDRIII amino acid identity in multiple donors) in our cohort. Such clonotypes were overall very rare, and most frequent in neonates and children <4 yr of age, in line with our previous observations (Budeus et al., 2020 Preprint). A marginal enrichment of IGHV-mutated clonotypes is detectable in young adults (Fig. 5, F and G).

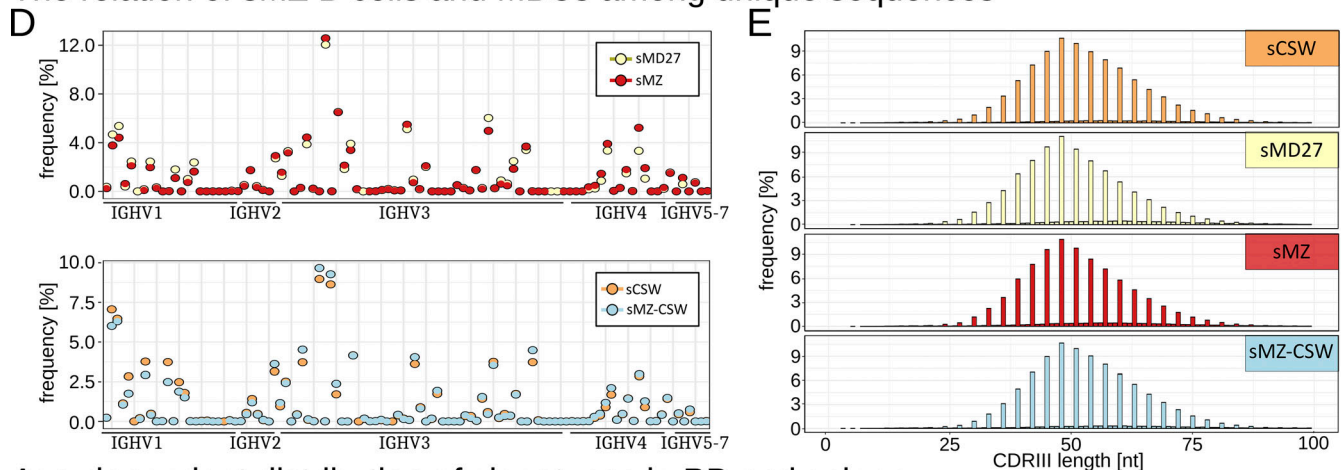
According to our analysis, human sMZ B cells represent a stochastic sample of the total MBC compartment. To validate the hypothesis that the CD21<sup>high</sup> sMZ B cell phenotype can be induced in MBCs or even antigen-naïve B cells, we made use of an established in vitro system for NOTCH2-dependent sMZ B cell development, which has previously been shown to affect the



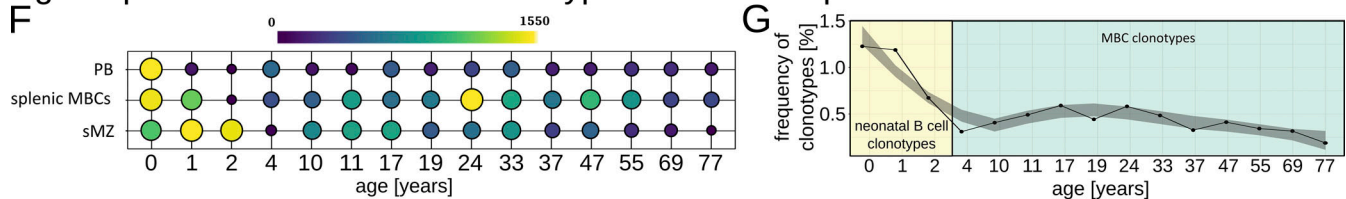
## The relation of sMZ B cells and MBCs among clones



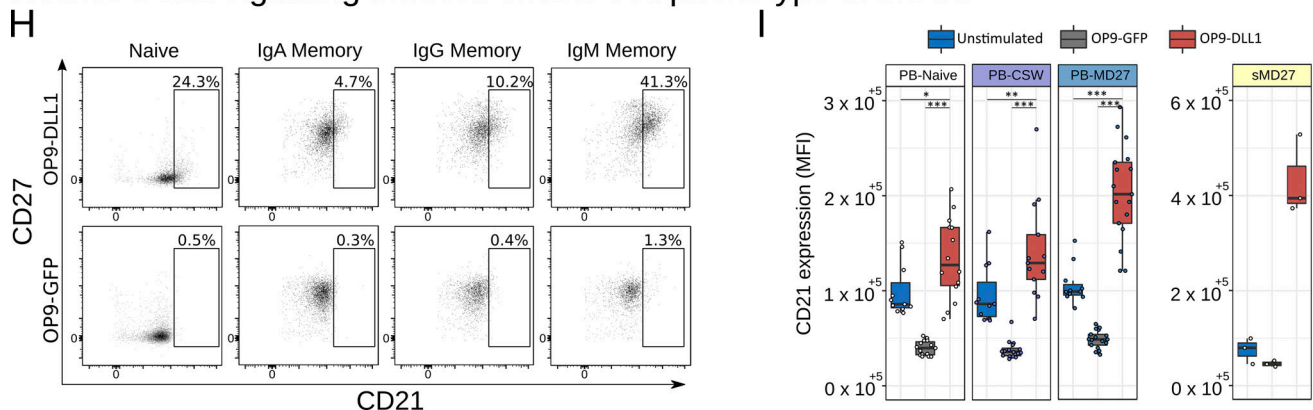
## The relation of sMZ B cells and MBCs among unique sequences



## Age-dependent distribution of clonotypes in PB and spleen



## Notch2-DLL1 signaling induces sMZ B cell phenotype in MBCs



**Figure 5. Molecular and functional characteristics of primed memory in the sMZ. (A)** Fraction of clonally related CD21<sup>high</sup>- and CD21<sup>+</sup>-derived sequences among all clones from 15 donors with sMD27 B cells available. **(B)** Examples of genealogical trees showing CD21<sup>high</sup>- and CD21<sup>+</sup>-derived sequences in alternating positions at consecutive nodes. **(C)** The frequency of dendrogram hierarchies among clonally related CD21<sup>high</sup>- and CD21<sup>+</sup>-derived sequences from all donors with more than five CD21<sup>high</sup> members in clones ( $n = 16$  donors). **(D)** Average IGHV-gene usage of sMZ and sMD27 (top), and sMZ-CSW and sCSW (bottom) subsets from 17 donors. IGHV genes are grouped according to the families 1–7. **(E)** Average CDRIII length distribution of splenic B cell subsets from 17 donors. **(F)** Enrichment of clonotypic sequences (defined by the same IGHV gene and at least 90% CDRIII amino acid similarity in multiple individuals) among sMZ (sMZ and sMZ-CSW pooled), splenic non-sMZ MBC (sMD27 and sCSW pooled), and PB-derived MBC (PB-MD27 and PB-CSW pooled) subsets. Absolute



number of clonotypes is given. **(G)** Clonotype frequency among all sequences from 15 donors with at least four available B cell subsets. Neonatal-derived clonotypes were retrieved from Budeus et al., and MBC-derived clonotypes were retrieved from Ig mutated sequences of class-switched B cells (Budeus et al., 2020 Preprint). The curve links the data points (gray area represents the 95% CI of the smoothed conditional means with loess fitting). **(H)** Representative fluorescence-activated cell scanning analysis of CD21 and CD27 surface expression of sort-purified PB-derived B cell subsets after 120 h of in vitro co-culture with either OP9-DLL1 (top row) or OP9-GFP (bottom row). **(I)** Surface CD21 expression (MFI) of naive B cells, PB-MD27, PB-CSW ( $n > 10$ ), and sMD27 ( $n = 3$ ) B cells after co-culture with OP9-DLL1, OP9-GFP, or unstimulated (before culture). Significance was calculated with the Wilcoxon rank-sum test (\*,  $P \leq 0.05$ ; \*\*,  $P \leq 0.005$ ; \*\*\*,  $P \leq 0.001$ ).

transcriptional program also (Descatoire et al., 2014). Under OP9-DLL1 stimulation in co-culture, PB-MD27 and PB-CSW B cells acquire a CD21<sup>high</sup> phenotype (Fig. 5, H and I). CD21<sup>high</sup> expression was more efficiently adopted by MBCs than naive B cells, especially by IgM-expressing MBCs (PB-MD27 and sMD27; Fig. 5 I). The CD21<sup>high</sup> phenotype is transient and dependent on the sustained presence of DLL1, as interruption of the co-culture or long-term cultivation of isolated sMZ B cells reverted their CD21<sup>high</sup> phenotype (not shown).

Taken together, human sMZ B cells show an extensive repertoire similarity to circulating and non-sMZ (CD21<sup>+</sup>) memory compartments.

## Discussion

The age-dependent dynamics of the human MBC repertoire are poorly investigated. Here, we present a phenotypical, molecular, and functional characterization of paired PB- and spleen-derived MBCs from healthy human subjects, covering eight decades of life.

In children >4 yr of age, the clonal relation of PB and splenic MBCs is already extensive. Even smallest MBC clones with only a single PB member nearly always had clone members in the spleen. This clonal relation of the PB and spleen B cell compartments is consistently detected in 14 donors analyzed. As only a small sample of the PB pool was tested, but was comprehensively covered by splenic relations, this suggests that members of nearly every MBC clone in the circulation may find their way into the spleen. Indeed, early in life, changes of clonal abundance and repertoire complexity are first detectable in PB and subsequently extend to the spleen. Thus, circulating MBCs egressing from GC-dependent maturation in secondary lymphoid organs, e.g., of the respiratory or gastrointestinal tract (Mamani-Matsuda et al., 2008; Mandric et al., 2020; Meng et al., 2017), channel into the splenic archive. Our study is not suitable to make reliable extrapolations to the size of individual clones (Friedensohn et al., 2018), as identical sequences were collapsed within each subset to reduce technical amplification bias. Moreover, we cannot quantify the degree to which primary diversification mechanisms contribute to dendrogram structures. We assume that early in life, where average mutation levels are low and class-switched MBCs are scarce, primary diversification might contribute to repertoire diversity (Scheeren et al., 2008; Weller et al., 2004; Weller et al., 2001; Weller et al., 2008). However, the strong increase of Ig mutation frequencies during late childhood, the frequent detection of consecutive (selected) mutations in clone dendrograms, and the existence of shared (IgM and class-switched) clone members argue for an antigen-dependent GC diversification (Budeus et al., 2015; Seifert and

Küppers, 2009). Upon generation and tissue egress, MBCs are comprehensively collected in the spleen, where the blood flow is slowed down and the splenic architecture supports adhesion, residence, and survival of MBCs (Lu and Cyster, 2002; Puga et al., 2011). We anticipate that in this way, from birth on, circulating MBCs build a systematic MBC archive in the spleen. This archive not only is comprehensively composed of clones with relation to the PB, but also produces and hosts a memory compartment without detectable members in the circulation. The fraction of sequences belonging to splenic clones increases with age.

Archive memory is not simply a storage, but its members are sampled for priming and immune surveillance in the sMZ microenvironment. As mutation load, IGHV gene usage, CDRIII distribution, and dendrogram patterns do not differ significantly between sMZ and corresponding non-sMZ B cell subsets, this sampling process is apparently random. We assume that the intermingling of sMZ and non-sMZ B cells is a strong indication for a constant oscillation between both archive compartments. Moreover, our data suggest a different generation and dynamics of human sMZ B cells than in mice, where numerous studies support the idea of a distinct sMZ B cell lineage with unique characteristics (Cariappa et al., 2001; Casola et al., 2004; Cerutti et al., 2013; Martin and Kearney, 2000; Pillai and Cariappa, 2009; Rickert et al., 1995). It was reported that in young children, a human sMZ precursor with commitment to an sMZ B cell phenotype and gene expression upon Notch2 signaling contributes to sMZ B cell development (Descatoire et al., 2014). This is supported and extended by our functional studies, showing that virtually all mature B cell subsets develop a CD21<sup>high</sup> phenotype upon DLL1 stimulation. Our molecular and functional analyses suggest that the distinctness of human sMZ B cells is not intrinsically encoded but may be imposed from the sMZ microenvironment.

Despite their distinct origins, human and murine sMZ B cells seem to share similar immunological functions, as the priming effect of the sMZ microenvironment is evident in humans also (Cerutti et al., 2013; Puga et al., 2011; Tangye et al., 1998), and we confirmed the primed state of CD21<sup>high</sup> sMZ versus CD21<sup>+</sup> splenic non-sMZ B cells and PB MBCs by their different responsiveness and proliferation capacity.

The phylogenetic analysis of shared clones between PB and spleen (sMZ and non-sMZ) indicates that the clonal relation is not entirely random, but often shows a highly ordered pattern. This pattern has two main features. First, circulating clone members often cluster in single, discrete branches of genealogic dendrograms, suggesting that the circulating MBCs adapted in secondary or tertiary GC reactions, and did not (yet?) reenter the splenic archive. Second, the PB branches originate further

downstream of the dendrogram root, suggesting that splenic and PB clone members often share their primary diversification and/or antigen-dependent selection history. Discrete PB branches are less frequent in infants (0 and 1 yr of age), but dominant in childhood and young adults (2–20 yr of age), and progressively decrease with age. The highly diversified, discrete branches of PB clones support the idea of reactivated splenic MBCs, likely representing reactivated sMZ B cells that have previously been described to circulate via the bloodstream (Weller et al., 2004). Thus, the circulating MBC compartment is composed of newly generated MBCs (or new primary diversified B lymphocytes), which have the ability to home to the splenic archive, but presumably also (re)activated sMZ and non-sMZ B cells that egressed from there. We assume that human PB B cells include recirculating sMZ B cells, which are detectable by immunogenetic features, but not phenotypical CD21<sup>high</sup> expression.

Finally, an increasing alternation between PB- and spleen-derived sequences in the dendrograms is detectable with age, arguing for increased recirculation between periphery and spleen, and for characteristic dynamics of the MBC system in humans.

The comparative analysis of MBC clone abundance, clone size (counting collapsed sequences deviating by at least one mutation), and isotype composition identified two major features of splenic clone members. First, splenic MBCs expand continuously with age, and thereby, larger clones outcompete smaller ones. Second, splenic B cell memory appears conservative, as clonal expansion is uncoupled from class-switching. IgM MBC and class-switched members are preserved equally. This contrasts with the circulating MBC compartment, which is shaped by an increase in Ig diversification and class-switching, as reported previously (Budeus et al., 2015; Seifert and Küppers, 2009; Seifert and Küppers, 2016; Seifert et al., 2015; Tangye et al., 2003; Tangye and Tarlinton, 2009).

The dynamics of circulating and archive memory (including sMZ B cells) provide insight into essential mechanisms of human immune aging. The infant spleen is predominantly composed of naive B cells, showing little indication for IGHV gene selection, GC-dependent diversification, or expanded MBC clones, although a large population of sMZ B cells is present. Around midlife, archive B cell clonality substantially increases, causing accumulation and persistence of large MBC clones in the elderly. As this occurs at the expense of smaller clones, it is likely increasingly difficult to archive new MBC clones in old age. These changes coincide with the time of thymic involution and changes in lymphopoiesis in the bone marrow (Guerrettaz et al., 2008; Palmer et al., 2018; Pang et al., 2011). We assume that the differences in Ig repertoires of infants and the elderly are a major cause of the increased susceptibility to infections in these risk groups, compared with young adults (Di Sabatino et al., 2011; Siegrist and Aspinall, 2009; Timens et al., 1989). We can only speculate that the predominance of sMZ-CSW in elderly individuals affects responsiveness to polysaccharide vaccines, enabling an effective secondary response to previously encountered antigens but preventing the formation of new memory. By contrast, conjugated polysaccharide vaccines provide T cell help and trigger memory formation arising from

naive B cells, albeit these decrease in the elderly. Thus, our findings might have direct implications for age-related immunization programs.

We propose here an updated view on the human MBC system, with a special emphasis on B cells in the spleen and their relation to PB MBCs. In this view, human B cell memory is composed of three compartments that are dynamically interwoven. Circulating MBCs carry traits of adaptive, evolving immune responses. Newly egressing MBCs are recruited into the spleen, where they contribute to a systematic MBC archive, which is homogeneously expanded and conserved throughout age. A random but frequently exchanging sample of archive memory is recruited into the primed or preactivated sMZ compartment (primed memory), forming a fast-responding subset of the splenic archive. Splenic MBCs can reenter circulation for further adaptation in the periphery (or the spleen itself). Human MBC composition changes with age; the outgrowth of many large clones in the spleen starts at mid-life and dominates immune aging, presumably being a prerequisite for enhanced lymphomagenesis and susceptibility to infection in the elderly.

## Materials and methods

### Human samples

Buffy coats were collected from PB donations of immunologically healthy human adults at the Institute for Transfusion Medicine at the Medical School Essen after informed consent was given according to the Declaration of Helsinki, as well as approval by the ethics committee of the Medical Faculty of the University of Duisburg-Essen, Germany. Splenic biopsies and paired PB were prepared on the same day from organ donors (Table S1). All samples were collected from leftover material from the Institute for Transfusion Medicine at the Medical School Essen, as approved by the ethics committee of the Medical Faculty of the University of Duisburg-Essen, Germany. All individuals died of noninfectious and nonmalignant causes, i.e., anoxic brain damage, cardiac arrest, cerebral trauma, bleeding, or infarction.

### Mononuclear cell isolation, magnetic cell separation, flow cytometry, and cell sorting

Mononuclear cells from different tissues were isolated by Ficoll density gradient centrifugation followed by positive selection of CD19-expressing cells by magnetic cell separation (Miltenyi Biotec).

B lymphocytes were either analyzed on a CytoFLEX S flow cytometer (Beckman Coulter) using the CytExpert software V2.4 (Beckman Coulter) or FlowJo Software V10.6.2, or sort-purified on a FACSARIA Fusion cell sorter or FACSARIA III cell sorter (BD Biosciences) equipped with BD FACSDiva software (BD Biosciences). For IGHV gene rearrangement analysis by high-throughput sequencing, the B cell subsets were sorted according to the following phenotypes: MBCs from PB were sorted as PB-MD27 (CD20<sup>+</sup>IgM<sup>+</sup>IgD<sup>+</sup>CD27<sup>+</sup>CD23<sup>−</sup>CD21<sup>+</sup>) or PB-CSW (CD20<sup>+</sup>IgG<sup>+</sup>/IgA<sup>+</sup>CD27<sup>+</sup>CD23<sup>−</sup>CD21<sup>+</sup>) B cells. Splenic B cell populations were sorted as sMZ (CD20<sup>+</sup>IgM<sup>+</sup>IgD<sup>+/−</sup>CD27<sup>+</sup>CD23<sup>−</sup>CD21<sup>high</sup>), sMZ-CSW (CD20<sup>+</sup>IgG<sup>+</sup>/IgA<sup>+</sup>

CD27<sup>+</sup>CD23<sup>-</sup>CD21<sup>high</sup>), sMD27 (CD20<sup>+</sup>IgM<sup>+</sup>IgD<sup>+/low</sup>CD27<sup>+</sup>CD23<sup>-</sup>CD21<sup>+</sup>), and sCSW (CD20<sup>+</sup>IgG<sup>+</sup>/IgA<sup>+</sup>CD27<sup>+</sup>CD23<sup>-</sup>CD21<sup>+</sup>) B cells. For in vitro functional assays, B cell subsets were sorted according to the following phenotypes: PB-Naive and sNaive B cells were sorted for functional validations (CD20<sup>+</sup>IgM<sup>low</sup>IgD<sup>high</sup>CD27<sup>-</sup>CD23<sup>+</sup>CD5<sup>-</sup>CD21<sup>+</sup>), PB-MD27 and sMD27 (CD20<sup>+</sup>IgM<sup>+</sup>IgD<sup>+/low</sup>CD27<sup>+</sup>CD23<sup>-</sup>CD21<sup>+</sup>), PB-CSW and sCSW (CD20<sup>+</sup>IgM<sup>-</sup>IgD<sup>-</sup>CD27<sup>+</sup>CD23<sup>-</sup>CD21<sup>+</sup>), sMZ (CD20<sup>+</sup>IgM<sup>+</sup>IgD<sup>+/low</sup>CD27<sup>-</sup>CD23<sup>-</sup>CD21<sup>high</sup>), and sMZ-CSW (CD20<sup>+</sup>IgM<sup>-</sup>IgD<sup>-</sup>CD27<sup>+</sup>CD23<sup>-</sup>CD21<sup>high</sup>).

### In vitro OP9 co-culture

OP9 co-culture assays were performed as described previously (Descatoire et al., 2014). Briefly, OP9-GFP or OP9-DLL1 stromal cells were seeded in 24-well plates at a density of 20,000 cells/well. After 24 h, sort-purified B cell subsets were added at a density of 50,000 cells/well, and after additional 5 d of incubation, cell surface expression of CD21 and CD27 was analyzed on a CytoFLEX S flow cytometer (Beckman Coulter) using the CytExpert software (Beckman Coulter).

### In vitro functional assays

For functional studies, human splenic B cell subsets (sMZ, sMD27, sCSW, sMZ-CSW, and sNaive) and PB B cell subsets (PB-MD27, PB-CSW, and PB-Naive) were isolated using fluorescence-activated cell sorting (FACS) and cultured in RPMI 1640 medium supplemented with 20% fetal bovine serum (Pan Biotech), 100 U/ml penicillin, and 100 µg/ml streptomycin at 37°C and 5% CO<sub>2</sub>. All populations were left unstimulated or were activated by TD stimulation using 0.03 µg/µl anti-Ig (Jackson ImmunoResearch) and 1 µg/ml CD40-ligand-hemagglutinin with 5 ng/ml anti-hemagglutinin antibodies (R&D Systems). TI-I stimulation was mimicked by incubation with 2.5 µM cytosine-phosphate-guanine oligonucleotide type B (InvivoGen). Phenotypic analyses were performed directly after cell sorting without further activation, and after 24 h of incubation in the presence of TI-I or TD stimulation. In proliferation assays, cells were pulsed with eFluor670 (Invitrogen) at a concentration of 5 µM, stimulated with TD or TI-I stimulation, and analyzed after 48, 72, and 96 h of incubation.

### IGHV gene rearrangement analysis by high-throughput sequencing

Rearranged IGHV genes of the sort-purified B cells were sequenced by next-generation sequencing. Genomic DNA was extracted from sorted B cell populations (Gentra Puregene Core Kit; Qiagen). Sequencing was performed using the Lympho-TrackDx IGH FR1 assay (Invivoscribe Inc.) and the rapid run program with paired-end sequencing and two times 300 bp read length. Reads generated by MiSeq (Illumina) were included only when the average quality was ≥25. Ambiguities between forward and reverse reads were replaced by “N.” Identical sequences were classified as PCR duplicates and reduced to the longest detected sequence. Each N in a given sequence was replaced by the most frequent (majority vote) nucleotide at that position. Only in-frame sequences detected more than once were further processed, as a means to filter out PCR errors or sequencing artifacts present in single sequences. Sequences were considered clonally related when using the same IGHV

gene and sharing at least 97% CDRIII sequence similarity and when sequences were derived from at least two B cell subsets. Clonally related sequences within single subsets (identified by intracлонаl Ig diversity) were disregarded due to their low frequency and probability of artificial origin. All analyses were performed with R 3.6 (<http://www.R-project.org>). The IGHV sequencing data are accessible under the BioProject ID PRJNA681128.

### Clonal abundance calculations

Clonal abundance (fraction of sequences belonging to clones) was calculated using a stochastically selected set of sequences with equal numbers of sequences from each sorted population (e.g., 40,000 sequences from sMZ from each donor, 4,800 sequences from PB-CSW from each donor). These reduced numbers were used to calculate clones to normalize for changes in clonal numbers due to different numbers of sorted, processed, and sequenced cells. All further analyses were performed with R 3.6, using several packages to visualize (ggplot2, ggpubr; circo plots: circlize; radar plots: fmsb; Gu et al., 2014; Kassambara, 2020; Nakazawa, 2019; Villanueva and Chen, 2019) and perform calculations, such as dose-response analyses (drc; Ritz et al., 2015).

### Calculation and analyses of hierarchical trees

Hierarchical trees of all sequences in clones were calculated for each donor using IgTree (Barak et al., 2008). Tree analyses and visualizations were performed in R using the packages igraph (Csárdi and Nepusz, 2006) and Rgraphviz (Hansen et al., 2020). Subtree analyses were performed in trees with five or more sequences of the cell population analyzed (e.g., five or more sequences originating from PB).

### Analyses of sequence characteristics

All evaluations were based on the international ImMunoGeneTics information system database (<http://www.imgt.org/>). Mutation frequencies were calculated based on the number of nucleotide exchanges in the IGHV region of each sequence in comparison with the most similar allelic variant present in the respective donor (determined from unmutated sequences). IGHV identification was performed with BLAST (<https://blast.ncbi.nlm.nih.gov/Blast.cgi>). CDRIII length distribution was calculated using the nucleotides covering the whole CDRIII as determined by the ImMunoGeneTics information system.

### Clonotype calculations

Clonotypes were analyzed using the amino acid sequence of the CDRIII and the information of the IGHV gene used. All sequences with at least 90% identity and the same IGHV gene regardless of their subset from at least two different donors were considered as a clonotype. Clonal expansions in clonotypes (sequences originating from the same donor) were excluded.

### Online supplemental material

Fig. S1 shows the gating strategy for PB and splenic B cell subsets and shows representative analyses of the age-related changes in the IgM and CD21 expression among PB and splenic B cells of five



individuals. It also shows the subset frequencies of PB B cell subsets and splenic CD21<sup>+</sup> MBCs. Fig. S2 shows the steady-state expression of differentiation markers, and steady-state and up-regulation of activation markers after 24 h of TI-I or TD in vitro stimulation. Fig. S3 shows the clonal fraction between all sequences. It also shows all clonal relations among all B cell subsets. Table S1 shows the donor characteristics and usage in figures. Table S2 shows the cells included in BCR deep sequencing and number of sequences retrieved by next-generation sequencing.

## Acknowledgments

We thank Klaus Lennartz for his valuable engineering support. We thank Ludger Klein-Hitpass and the staff members at the Biochip Laboratory at the Institute of Cell Biology in Essen. We thank the staff members at the flow cytometry and fluorescence core facility Imaging Center Essen.

This work was supported by the Deutsche Forschungsgemeinschaft through grants SE1885/2-1, SE1885/2-2, and SE1885/4-1 and the Deutsche Krebshilfe through grant 70112628.

Author contributions: A. Kibler designed and carried out most of the experiments and prepared the manuscript. B. Budeus developed and performed bioinformatical and statistical analysis. E. Homp, K. Bronischewski, V. Berg, L. Sellmann, F. Murke, A. Heinold, F.M. Heinemann, M. Lindemann, I. Beker-edjian-Ding, C. Kirschning, and P.A. Horn contributed experimental work and provided material. R. Küppers, B. Budeus, and M. Seifert developed the concept, designed experimental strategies, helped with data evaluation, and prepared the manuscript.

Disclosures: The authors declare no competing interests exist.

Submitted: 9 September 2020

Revised: 2 November 2020

Accepted: 21 December 2020

## References

Arnon, T.I., R.M. Horton, I.L. Grigorova, and J.G. Cyster. 2013. Visualization of splenic marginal zone B-cell shuttling and follicular B-cell egress. *Nature*. 493:684–688. <https://doi.org/10.1038/nature11738>

Bagnara, D., M. Squillario, D. Kipling, T. Mora, A.M. Walczak, L. Da Silva, S. Weller, D.K. Dunn-Walters, J.C. Weill, and C.A. Reynaud. 2015. A Re-assessment of IgM Memory Subsets in Humans. *J. Immunol.* 195: 3716–3724. <https://doi.org/10.4049/jimmunol.1500753>

Barak, M., N.S. Zuckerman, H. Edelman, R. Unger, and R. Mehr. 2008. Ig-Tree: creating Immunoglobulin variable region gene lineage trees. *J. Immunol. Methods*. 338:67–74. <https://doi.org/10.1016/j.jim.2008.06.006>

Budeus, B., S. Schweigle de Reynoso, M. Przekopowicz, D. Hoffmann, M. Seifert, and R. Küppers. 2015. Complexity of the human memory B-cell compartment is determined by the versatility of clonal diversification in germinal centers. *Proc. Natl. Acad. Sci. USA*. 112:E5281–E5289. <https://doi.org/10.1073/pnas.1511270112>

Budeus, B., A. Kibler, M. Brauser, E. Homp, K. Bronischewski, J.A. Ross, A. Görgens, M.A. Weniger, J. Dunst, T. Kreslavsky, et al. 2020. Human neonatal B cell immunity differs from the adult version by conserved Ig repertoires and rapid, but transient response dynamics. *bioRxiv*. <https://doi.org/10.1101/2020.08.11.245985> (Preprint posted September 10, 2020)

Cariappa, A., M. Tang, C. Parng, E. Nebelitskiy, M. Carroll, K. Georgopoulos, and S. Pillai. 2001. The follicular versus marginal zone B lymphocyte cell fate decision is regulated by Aiolos, Btk, and CD21. *Immunity*. 14: 603–615. [https://doi.org/10.1016/S1074-7613\(01\)00135-2](https://doi.org/10.1016/S1074-7613(01)00135-2)

Casola, S., K.L. Otipoby, M. Alimzhanov, S. Humme, N. Uyttersprot, J.L. Kutok, M.C. Carroll, and K. Rajewsky. 2004. B cell receptor signal strength determines B cell fate. *Nat. Immunol.* 5:317–327. <https://doi.org/10.1038/ni1036>

Cerutti, A., M. Cols, and I. Puga. 2013. Marginal zone B cells: virtues of innate-like antibody-producing lymphocytes. *Nat. Rev. Immunol.* 13:118–132. <https://doi.org/10.1038/nri3383>

Cinamon, G., M.A. Zachariah, O.M. Lam, F.W. Foss Jr., and J.G. Cyster. 2008. Follicular shuttling of marginal zone B cells facilitates antigen transport. *Nat. Immunol.* 9:54–62. <https://doi.org/10.1038/ni1542>

Colombo, M., G. Cutrona, D. Reverberi, S. Bruno, F. Ghiotto, C. Tenca, K. Stamatopoulos, A. Hadzidimitriou, J. Ceccarelli, S. Salvi, et al. 2013. Expression of immunoglobulin receptors with distinctive features indicating antigen selection by marginal zone B cells from human spleen. *Mol. Med.* 19:294–302. <https://doi.org/10.2119/molmed.2013.00069>

Csárdi, G., and T. Nepusz. 2006. The igraph software package for complex network research (R package version 0.8.2). *InterJournal Complex Systems*. 1695:1–9.

De Silva, N.S., and U. Klein. 2015. Dynamics of B cells in germinal centres. *Nat. Rev. Immunol.* 15:137–148. <https://doi.org/10.1038/nri3804>

Descatoire, M., S. Weller, S. Irtan, S. Sarnacki, J. Feuillard, S. Storck, A. Guiochon-Mantel, J. Bouligand, A. Morali, J. Cohen, et al. 2014. Identification of a human splenic marginal zone B cell precursor with NOTCH2-dependent differentiation properties. *J. Exp. Med.* 211:987–1000. <https://doi.org/10.1084/jem.20132203>

Di Sabatino, A., R. Carsetti, and G.R. Corazza. 2011. Post-splenectomy and hyposplenic states. *Lancet*. 378:86–97. [https://doi.org/10.1016/S0140-6736\(10\)61493-6](https://doi.org/10.1016/S0140-6736(10)61493-6)

Dogan, I., B. Bertocci, V. Vilmon, F. Delbos, J. Mégret, S. Storck, C.A. Reynaud, and J.C. Weill. 2009. Multiple layers of B cell memory with different effector functions. *Nat. Immunol.* 10:1292–1299. <https://doi.org/10.1038/ni.1814>

Dono, M., S. Zupo, N. Leanza, G. Melioli, M. Fogli, A. Melagrana, N. Chiorazzi, and M. Ferrarini. 2000. Heterogeneity of tonsillar subepithelial B lymphocytes, the splenic marginal zone equivalents. *J. Immunol.* 164: 5596–5604. <https://doi.org/10.4049/jimmunol.164.11.5596>

Dunn-Walters, D.K., P.G. Isaacson, and J. Spencer. 1995. Analysis of mutations in immunoglobulin heavy chain variable region genes of microdissected marginal zone (MGZ) B cells suggests that the MGZ of human spleen is a reservoir of memory B cells. *J. Exp. Med.* 182:559–566. <https://doi.org/10.1084/jem.182.2.559>

Ettinger, R., G.P. Sims, R. Robbins, D. Withers, R.T. Fischer, A.C. Grammer, S. Kuchen, and P.E. Lipsky. 2007. IL-21 and BAFF/BLyS synergize in stimulating plasma cell differentiation from a unique population of human splenic memory B cells. *J. Immunol.* 178:2872–2882. <https://doi.org/10.4049/jimmunol.178.5.2872>

Friedensohn, S., J.M. Lindner, V. Cornacchione, M. Iazeolla, E. Miho, A. Zingg, S. Meng, E. Traggiai, and S.T. Reddy. 2018. Synthetic Standards Combined With Error and Bias Correction Improve the Accuracy and Quantitative Resolution of Antibody Repertoire Sequencing in Human Naïve and Memory B Cells. *Front. Immunol.* 9:1401. <https://doi.org/10.3389/fimmu.2018.01401>

Gibson, K.L., Y.C. Wu, Y. Barnett, O. Duggan, R. Vaughan, E. Kondeatis, B.O. Nilsson, A. Wikby, D. Kipling, and D.K. Dunn-Walters. 2009. B-cell diversity decreases in old age and is correlated with poor health status. *Aging Cell*. 8:18–25. <https://doi.org/10.1111/j.1474-9726.2008.00443.x>

Giesecke, C., D. Frölich, K. Reiter, H.E. Mei, I. Wirries, R. Kuhly, M. Killig, T. Glatzer, K. Stölzel, C. Perka, et al. 2014. Tissue distribution and dependence of responsiveness of human antigen-specific memory B cells. *J. Immunol.* 192:3091–3100. <https://doi.org/10.4049/jimmunol.1302783>

Gu, Z., L. Gu, R. Eils, M. Schlesner, and B. Brors. 2014. circlize Implements and enhances circular visualization in R. *Bioinformatics*. 30:2811–2812. <https://doi.org/10.1093/bioinformatics/btu393>

Guerretaz, L.M., S.A. Johnson, and J.C. Cambier. 2008. Acquired hematopoietic stem cell defects determine B-cell repertoire changes associated with aging. *Proc. Natl. Acad. Sci. USA*. 105:11898–11902. <https://doi.org/10.1073/pnas.0805498105>

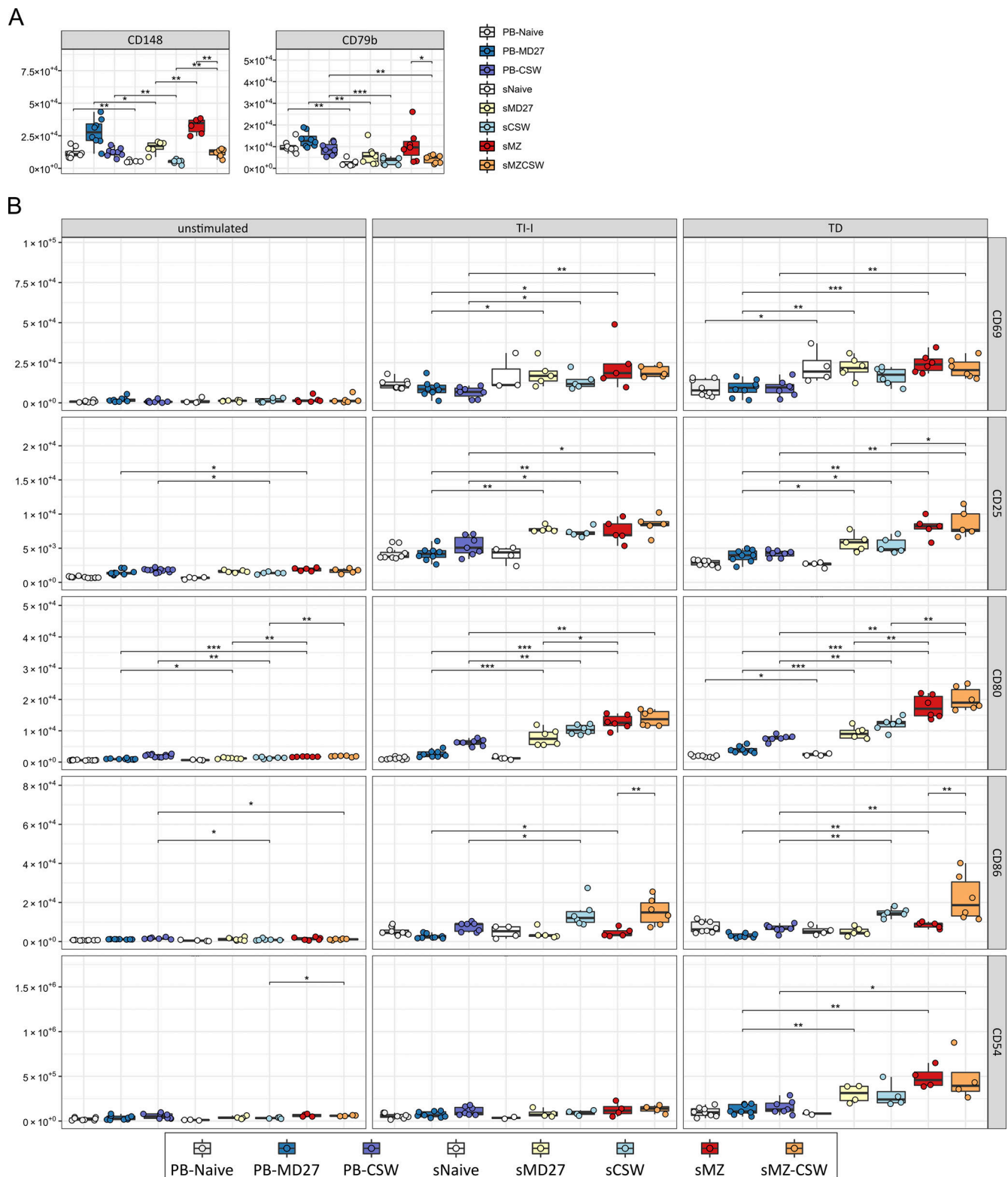
Hampel, F., S. Ehrenberg, C. Hojer, A. Draeseke, G. Marschall-Schröter, R. Kühn, B. Mack, O. Gires, C.J. Vahl, M. Schmidt-Suppran, et al. 2011. CD19-independent instruction of murine marginal zone B-cell development

- by constitutive Notch2 signaling. *Blood*. 118:6321–6331. <https://doi.org/10.1182/blood-2010-12-325944>
- Hansen, K., J. Gentry, L. Long, R. Gentleman, S. Falcon, F. Hahne, and D. Sarkar. 2020. Rgraphviz: Provides plotting capabilities for R graph objects. (R package version 2.32.0). <https://bioconductor.org/packages/release/bioc/html/Rgraphviz.html> (accessed September 8, 2020)
- Höfer, T., G. Muehlinghaus, K. Moser, T. Yoshida, H. E. Mei, K. Hebel, A. Hauser, B. Hoyer, E. O. Luger, T. Dörner, et al. 2006. Adaptation of humoral memory. *Immunol. Rev.* 211:295–302. <https://doi.org/10.1111/j.0105-2896.2006.00380.x>
- Kassambara, A. 2020. ggpubr: 'ggplot2' Based Publication Ready Plots (R package version 0.4.0). <https://rdrr.io/cran/ggpubr/> (accessed September 8, 2020)
- Kraal, G. 1992. Cells in the marginal zone of the spleen. *Int. Rev. Cytol.* 132: 31–74. [https://doi.org/10.1016/S0074-7696\(08\)62453-5](https://doi.org/10.1016/S0074-7696(08)62453-5)
- Kruetzmann, S., M.M. Rosado, H. Weber, U. Germing, O. Tournilhac, H.H. Peter, R. Berner, A. Peters, T. Boehm, A. Plebani, et al. 2003. Human immunoglobulin M memory B cells controlling *Streptococcus pneumoniae* infections are generated in the spleen. *J. Exp. Med.* 197:939–945. <https://doi.org/10.1084/jem.20022020>
- Lettau, M., A. Wiedemann, E.V. Schrezenmeier, C. Giesecke-Thiel, and T. Dörner. 2020. Human CD27+ memory B cells colonize a superficial follicular zone in the palatine tonsils with similarities to the spleen. A multicolor immunofluorescence study of lymphoid tissue. *PLoS One*. 15: e0229778. <https://doi.org/10.1371/journal.pone.0229778>
- Lu, T.T., and J.G. Cyster. 2002. Integrin-mediated long-term B cell retention in the splenic marginal zone. *Science*. 297:409–412. <https://doi.org/10.1126/science.1071632>
- Magri, G., M. Miyajima, S. Bascones, A. Mortha, I. Puga, L. Cassis, C.M. Barra, L. Comerma, A. Chudnovskiy, M. Gentile, et al. 2014. Innate lymphoid cells integrate stromal and immunological signals to enhance antibody production by splenic marginal zone B cells. *Nat. Immunol.* 15:354–364. <https://doi.org/10.1038/ni.2830>
- Mamani-Matsuda, M., A. Cosma, S. Weller, A. Faili, C. Staib, L. Garçon, O. Hermine, O. Beyne-Rauzy, C. Fieschi, J.O. Pers, et al. 2008. The human spleen is a major reservoir for long-lived vaccinia virus-specific memory B cells. *Blood*. 111:4653–4659. <https://doi.org/10.1182/blood-2007-11-123844>
- Mandric, I., J. Rotman, H.T. Yang, N. Strauli, D.J. Montoya, W. Van Der Wey, J.R. Ronas, B. Statz, D. Yao, V. Petrova, et al. 2020. Profiling immunoglobulin repertoires across multiple human tissues using RNA sequencing. *Nat. Commun.* 11:3126. <https://doi.org/10.1038/s41467-020-16857-7>
- Martin, F., and J.F. Kearney. 2000. Positive selection from newly formed to marginal zone B cells depends on the rate of clonal production, CD19, and btk. *Immunity*. 12:39–49. [https://doi.org/10.1016/S1074-7613\(00\)80157-0](https://doi.org/10.1016/S1074-7613(00)80157-0)
- Martin, F., and J.F. Kearney. 2002. Marginal-zone B cells. *Nat. Rev. Immunol.* 2:323–335. <https://doi.org/10.1038/nri799>
- Martin, F., A.M. Oliver, and J.F. Kearney. 2001. Marginal zone and B1 B cells unite in the early response against T-independent blood-borne particulate antigens. *Immunity*. 14:617–629. [https://doi.org/10.1016/S1074-7613\(01\)00129-7](https://doi.org/10.1016/S1074-7613(01)00129-7)
- McHeyzer-Williams, L.J., P.J. Milpied, S.L. Okitsu, and M.G. McHeyzer-Williams. 2015. Class-switched memory B cells remodel BCRs within secondary germinal centers. *Nat. Immunol.* 16:296–305. <https://doi.org/10.1038/ni.3095>
- Mebius, R.E., and G. Kraal. 2005. Structure and function of the spleen. *Nat. Rev. Immunol.* 5:606–616. <https://doi.org/10.1038/nri1669>
- Meng, W., B. Zhang, G.W. Schwartz, A.M. Rosenfeld, D. Ren, J.J.C. Thome, D.J. Carpenter, N. Matsuoka, H. Lerner, A.L. Friedman, et al. 2017. An atlas of B-cell clonal distribution in the human body. *Nat. Biotechnol.* 35: 879–884. <https://doi.org/10.1038/nbt.3942>
- Mesin, L., J. Ersching, and G.D. Victora. 2016. Germinal Center B Cell Dynamics. *Immunity*. 45:471–482. <https://doi.org/10.1016/j.immuni.2016.09.001>
- Nakazawa, M. 2019. fmsb: Functions for Medical Statistics Book with some Demographic Data (R package version 0.7.0). <https://rdrr.io/cran/fmsb/> (accessed September 8, 2020)
- Palmer, S., L. Albergante, C.C. Blackburn, and T.J. Newman. 2018. Thymic involution and rising disease incidence with age. *Proc. Natl. Acad. Sci. USA*. 115:1883–1888. <https://doi.org/10.1073/pnas.1714478115>
- Pang, W.W., E.A. Price, D. Sahoo, I. Beerman, W.J. Maloney, D.J. Rossi, S.L. Schrier, and I.L. Weissman. 2011. Human bone marrow hematopoietic stem cells are increased in frequency and myeloid-biased with age. *Proc. Natl. Acad. Sci. USA*. 108:20012–20017. <https://doi.org/10.1073/pnas.1116110108>
- Pillai, S., and A. Cariappa. 2009. The follicular versus marginal zone B lymphocyte cell fate decision. *Nat. Rev. Immunol.* 9:767–777. <https://doi.org/10.1038/nri2656>
- Puga, I., M. Cols, C.M. Barra, B. He, L. Cassis, M. Gentile, L. Comerma, A. Chorny, M. Shan, W. Xu, et al. 2011. B cell-helper neutrophils stimulate the diversification and production of immunoglobulin in the marginal zone of the spleen. *Nat. Immunol.* 13:170–180. <https://doi.org/10.1038/ni.2194>
- Rickert, R.C., K. Rajewsky, and J. Roes. 1995. Impairment of T-cell-dependent B-cell responses and B-1 cell development in CD19-deficient mice. *Nature*. 376:352–355. <https://doi.org/10.1038/376352a0>
- Ritz, C., F. Baty, J.C. Streibig, and D. Gerhard. 2015. Dose-Response Analysis Using R. *PLoS One*. 10:e0146021. <https://doi.org/10.1371/journal.pone.0146021>
- Scheeren, F.A., M. Nagasawa, K. Weijer, T. Cupedo, J. Kirberg, N. Legrand, and H. Spits. 2008. T cell-independent development and induction of somatic hypermutation in human IgM+ IgD+ CD27+ B cells. *J. Exp. Med.* 205:2033–2042. <https://doi.org/10.1084/jem.20070447>
- Seifert, M., and R. Küppers. 2009. Molecular footprints of a germinal center derivation of human IgM+(IgD+)CD27+ B cells and the dynamics of memory B cell generation. *J. Exp. Med.* 206:2659–2669. <https://doi.org/10.1084/jem.20091087>
- Seifert, M., and R. Küppers. 2016. Human memory B cells. *Leukemia*. 30: 2283–2292. <https://doi.org/10.1038/leu.2016.226>
- Seifert, M., M. Przekopowicz, S. Taudien, A. Lollies, V. Ronge, B. Drees, M. Lindemann, U. Hillen, H. Engler, B.B. Singer, and R. Küppers. 2015. Functional capacities of human IgM memory B cells in early inflammatory responses and secondary germinal center reactions. *Proc. Natl. Acad. Sci. USA*. 112:E546–E555. <https://doi.org/10.1073/pnas.1416276112>
- Siegrist, C.A., and R. Aspinall. 2009. B-cell responses to vaccination at the extremes of age. *Nat. Rev. Immunol.* 9:185–194. <https://doi.org/10.1038/nri2508>
- Sintes, J., M. Gentile, S. Zhang, Y. Garcia-Carmona, G. Magri, L. Cassis, D. Segura-Garzon, A. Ciociola, E.K. Grasset, S. Bascones, et al. 2017. mTOR intersects antibody-inducing signals from TAC1 in marginal zone B cells. *Nat. Commun.* 8:1462. <https://doi.org/10.1038/s41467-017-01602-4>
- Song, H., and J. Cerny. 2003. Functional heterogeneity of marginal zone B cells revealed by their ability to generate both early antibody-forming cells and germinal centers with hypermutation and memory in response to a T-dependent antigen. *J. Exp. Med.* 198:1923–1935. <https://doi.org/10.1084/jem.20031498>
- Steiniger, B.S. 2015. Human spleen microanatomy: why mice do not suffice. *Immunology*. 145:334–346. <https://doi.org/10.1111/imm.12469>
- Steiniger, B., and P. Barth. 2000. Microanatomy and function of the spleen. *Adv. Anat. Embryol. Cell Biol.* 151:III–IX: 1–101.
- Steiniger, B., E.M. Timphus, R. Jacob, and P.J. Barth. 2005. CD27+ B cells in human lymphatic organs: re-evaluating the splenic marginal zone. *Immunology*. 116:429–442. <https://doi.org/10.1111/j.1365-2567.2005.02242.x>
- Steiniger, B.S., V. Wilhelmi, A. Seiler, K. Lampp, and V. Stachniss. 2014. Heterogeneity of stromal cells in the human splenic white pulp. Fibroblastic reticulum cells, follicular dendritic cells and a third superficial stromal cell type. *Immunology*. 143:462–477. <https://doi.org/10.1111/imm.12325>
- Tangye, S.G., and D.M. Tarlinton. 2009. Memory B cells: effectors of long-lived immune responses. *Eur. J. Immunol.* 39:2065–2075. <https://doi.org/10.1002/eji.200939531>
- Tangye, S.G., Y.J. Liu, G. Aversa, J.H. Phillips, and J.E. de Vries. 1998. Identification of functional human splenic memory B cells by expression of CD148 and CD27. *J. Exp. Med.* 188:1691–1703. <https://doi.org/10.1084/jem.188.9.1691>
- Tangye, S.G., D.T. Avery, E.K. Deenick, and P.D. Hodgkin. 2003. Intrinsic differences in the proliferation of naive and memory human B cells as a mechanism for enhanced secondary immune responses. *J. Immunol.* 170: 686–694. <https://doi.org/10.4049/jimmunol.170.2.686>
- Tanigaki, K., H. Han, N. Yamamoto, K. Tashiro, M. Ikegawa, K. Kuroda, A. Suzuki, T. Nakano, and T. Honjo. 2002. Notch-RBP-J signaling is involved in cell fate determination of marginal zone B cells. *Nat. Immunol.* 3:443–450. <https://doi.org/10.1038/ni793>
- Tierens, A., J. Delabie, L. Michiels, P. Vandenbergh, and C. De Wolf-Peters. 1999. Marginal-zone B cells in the human lymph node and spleen show

- somatic hypermutations and display clonal expansion. *Blood*. 93: 226–234. <https://doi.org/10.1182/blood.V93.1.226>
- Timens, W., A. Boes, T. Rozeboom-Uiterwijk, and S. Poppema. 1989. Immaturity of the human splenic marginal zone in infancy. Possible contribution to the deficient infant immune response. *J. Immunol.* 143:3200–3206.
- Villanueva, R.A.M., and Z.J. Chen. 2019. ggplot2: Elegant Graphics for Data Analysis. *Measurement*. 17:160–167. <https://doi.org/10.1080/15366367.2019.1565254>
- Wasserstrom, H., J. Bussel, L.C. Lim, and C. Cunningham-Rundles. 2008. Memory B cells and pneumococcal antibody after splenectomy. *J. Immunol.* 181:3684–3689. <https://doi.org/10.4049/jimmunol.181.5.3684>
- Weisel, F., and M. Shlomchik. 2017. Memory B Cells of Mice and Humans. *Annu. Rev. Immunol.* 35:255–284. <https://doi.org/10.1146/annurev-immunol-041015-055531>
- Weller, S., A. Faili, C. Garcia, M.C. Braun, F. Le Deist F, G. de Saint Basile G, O. Hermine, A. Fischer, C.A. Reynaud, and J.C. Weill. 2001. CD40-CD40L independent Ig gene hypermutation suggests a second B cell diversification pathway in humans. *Proc. Natl. Acad. Sci. USA*. 98:1166–1170. <https://doi.org/10.1073/pnas.98.3.1166>
- Weller, S., M.C. Braun, B.K. Tan, A. Rosenwald, C. Cordier, M.E. Conley, A. Plebani, D.S. Kumararatne, D. Bonnet, O. Tournilhac, et al. 2004. Human blood IgM “memory” B cells are circulating splenic marginal zone B cells harboring a prediversified immunoglobulin repertoire. *Blood*. 104:3647–3654. <https://doi.org/10.1182/blood-2004-01-0346>
- Weller, S., M. Mamani-Matsuda, C. Picard, C. Cordier, D. Lecoche, F. Gauthier, J.C. Weill, and C.A. Reynaud. 2008. Somatic diversification in the absence of antigen-driven responses is the hallmark of the IgM+ IgD+ CD27+ B cell repertoire in infants. *J. Exp. Med.* 205:1331–1342. <https://doi.org/10.1084/jem.20071555>
- Wen, L., J. Brill-Dashoff, S.A. Shinton, M. Asano, R.R. Hardy, and K. Hayakawa. 2005. Evidence of marginal-zone B cell-positive selection in spleen. *Immunity*. 23:297–308. <https://doi.org/10.1016/j.immuni.2005.08.007>
- Willenbrock, K., B. Jungnickel, M.L. Hansmann, and R. Küppers. 2005. Human splenic marginal zone B cells lack expression of activation-induced cytidine deaminase. *Eur. J. Immunol.* 35:3002–3007. <https://doi.org/10.1002/eji.200535134>
- Wu, Y.C., D. Kipling, H.S. Leong, V. Martin, A.A. Ademokun, and D.K. Dunn-Walters. 2010. High-throughput immunoglobulin repertoire analysis distinguishes between human IgM memory and switched memory B-cell populations. *Blood*. 116:1070–1078. <https://doi.org/10.1182/blood-2010-03-275859>
- Zhao, Y., M. Uduman, J.H.Y. Siu, T.J. Tull, J.D. Sanderson, Y.B. Wu, J.Q. Zhou, N. Petrov, R. Ellis, K. Todd, et al. 2018. Spatiotemporal segregation of human marginal zone and memory B cell populations in lymphoid tissue. *Nat. Commun.* 9:3857. <https://doi.org/10.1038/s41467-018-06089-1>







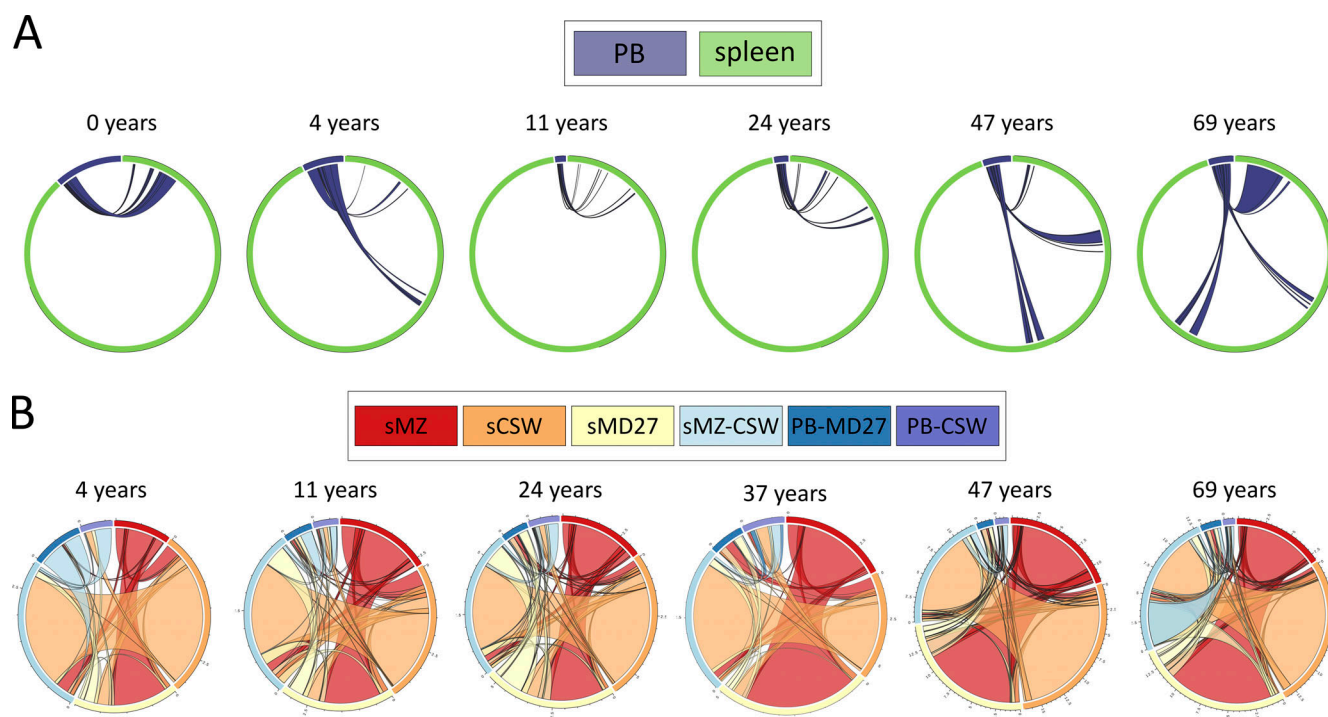


Figure S3. **Clonal relations between PB and spleen, and PB and splenic B cell subsets.** **(A)** Circos plots of clonally related sequences between PB and spleen among all sequences. **(B)** Circos plots of clonally related sequences between B cell subsets from PB and spleen are shown as ribbons among all clonally related sequences. A representative selection of six donors is shown.

Table S1 and Table S2 are provided online as separate Excel files. Table S1 shows donor characteristics and an overview of donors and usage in figures. Table S2 shows cells included in BCR deep sequencing and number of sequences retrieved by next-generation sequencing.